Spectroscopic and luminescent properties of Ce^{3+}-doped TeO_2-WO_3-GeO_2 glasses

G. Pullaiah [a], K. Venkata Rao [b,*], B.C. Jamalaiah [c,*], N. Madhu [d], Venkatramaiah Nutalapati [e,**]

[a] Department of Physics, Yogi Vemana University, Vemana Puram-516005, Andhra Pradesh, India
[b] Department of Physics, Government Degree College, Porumamilla-516193, Andhra Pradesh, India
[c] Department of Physics, Rajeev Gandhi Memorial College of Engineering and Technology (Autonomous), Nandyal-518501, Andhra Pradesh, India
[d] Department of Physics, P.R.R. & V.S. Government Degree College, Vidavaluru-524318, Andhra Pradesh, India
[e] Department of Chemistry, Faculty of Engineering and Technology, S.R.M. Institute of Science and Technology (SRM IST), Kattankulathur-603203, Tamil Nadu, India

ARTICLE INFO

ABSTRACT

Different concentrations of Ce^{3+}-doped TeO_2-WO_3-GeO_2-Ce_2O_3 (TWGCe) glasses were prepared by melt-quenching method and characterized. Different spectroscopic and luminescence properties were evaluated using room temperature absorption and emission spectra. The absence of sharp X-ray diffraction peaks and the presence of broad band from 18° to 35° shows the amorphous phase of studied glasses. The Fourier transform infrared absorption spectra show the presence of various vibrational bonds. The optical properties of TWGCe glasses were studied by exciting the glass samples at 323 nm ultraviolet wavelength. The quenching in luminescence is noticed at $\times = 0.5$ mol% along with a red-shift at higher Ce^{3+} concentrations. The decay time was found decrease with increase of concentration of Ce^{3+} ions. These glasses emit intense blue luminescence with CIE coordinates (0.161, 0.018) when excited at 323 nm radiation. These glasses are favourable as blue light sources in the design of phosphor-based white LEDs.

1. Introduction

The multi-component glasses are of most significant compared to single crystals. They are of interest due to their low fabrication cost, flexibility in manufacturing different sizes and shapes. The glassy materials have been used to produce various optical components with excellent transparency. They exhibit intense emission in near ultraviolet and visible regions, possesses relatively high density and more rare earth (RE) ion solubility [1–4]. They have tremendous applications as host materials for variety of RE ions doped laser sources, fiber amplifiers in communication, dispersion-control devices, sensors in industry, scintillators in radio-physics, etc…[5,6]. The trivalent cerium (Ce^{3+}) ions are the most commonly used REs for intense luminescence in the spectral range of 300–600 nm. These are most significant in designing oxide-based scintillators owing to their high fluorescence yield strength and short lifetime of the order of $10^{-8} – 10^{-9}$ s. The Ce^{3+}-doped scintillators find wide range of applications in the fields of bio-imaging, defense, communication and high-energy physics [7,8]. The emission of strong blue light from Ce^{3+} activated multi-component glass or glass-ceramics have been used to generate white light in phosphor based white light emitting diodes (w-LEDs) [9,10].

The tellurite-based glasses are of noteworthy due to their excellent non-linear optical properties with low phonon energy, relatively good thermal stability with chemical durability, low manufacturing temperature. These glasses are more advantages in enhancing the fluorescence efficiency by reducing multi-phonon relaxations rates [11,12]. The presence of TeO_4, TeO_{3+1}/TeO_3, WO_6, WO_4 and GeO_6 structural units which help in strengthening glass network, glass forming ability and hence thermal stability. The structural, physical and thermal properties [13] and the shielding properties [14] of TeO_2-WO_3-GeO_2 glasses have been studied. Certain RE^{3+} ions activated TeO_2-WO_3-GeO_2 glasses were fabricated and characterized for various visible and fiber laser sources [15–17]. This work reports on the structural and photoluminescence properties of TeO_2-WO_3-GeO_2-CeO_2 (TWGCe) glasses. The optimization of Ce^{3+} concentration and photometric properties were also discussed.

---

2. Materials, method of preparation and instrumentation

The TWGCex glasses of composition (85-x) TeO$_2$-5 WO$_3$-10 GeO$_2$-x Ce$_2$O$_3$ (x = 0, 0.1, 0.5 and 1.0 mol%) were prepared by melt-quenching method using TeO$_2$ ($\geq$99.5 %), WO$_3$($\geq$99 %), GeO$_2$(99.999 %) and Ce$_2$O$_3$(99.9 %) as precursor materials. The stoichiometric amounts of precursor materials of 20 g batch each were thoroughly mixed in the presence of acetone and melted at 875 °C for 40 min using alumina crucible. The melt was air-quenched by pouring onto a preheated brass mould and annealed at 300 °C for 10 h and then cooled to room temperature producing bubble-free and transparent glasses (see Fig. 1a). All these glass samples were polished for optical quality with 0.18 cm thick and then used for other characterizations. The prepared glass samples were referred as TWGCex glasses, where $\times$ stands for the concentration of Ce^{3+} ions in mol%.

The Archimedes principle was applied to obtain density measurements using double-distilled water as an immersion-fluid. The Abbes' refractometer illuminated with sodium vapour lamp (λ = 5893 Å) was used to find the refractive indices. The room temperature optical absorption spectra were recorded on Agilent Cary 60 UV–Visible spectrometer. The transmittance mode infrared absorption spectra were recorded with PerkinElmer FT-IR spectrometer following KBr technique. The scanning electron microscopy-energy dispersive X-ray spectrum (SEM-EDS) was recorded on VEGA3 TESCAN provided with BrukerEasy EDS equipment. The excitation and emission spectra were carried out with Jobin Yvon Fluorolog-3 spectrofluorimeter and the lifetime measurements were done using FLS 1000 photoluminescence spectrometer with light source in pulsed mode. All the optical measurements were performed at room temperature.

3. Results and discussion

3.1. Basic characteristic parameters

The phase of TWGCex glasses has been examined by powder X-ray diffraction (XRD) studies. The XRD profiles shown in Fig. 1b reveal a broad-bump range from 18° to 35° and it has been assigned to the combined effect of multiple-scatterings at non-uniformly distributed atoms leading to exhibit amorphous phase of studied glasses. Some of the significant basic parameters of TWGCex glasses are summarized in Table 1. The values of refractive index (n) and density (d) increase with increase of Ce^{3+} concentration and their variation are illustrated in Fig. 2. The decrease in molar volume (V$_m$) with Ce^{3+} concentration leads compactness of elements. The reflection loss is found to be ~ 18 % for all the samples indicating negligible loss of incident light intensity or the studied glasses allow most of the incident light to absorb or transmit through them. The ratio of molar refraction (R$_m$) to molar volume (V$_m$) has been used to predict metallic or non-metallic behaviour of glass samples. (R$_m$/V$_m$) > 1 for metallic nature of solids while (R$_m$/V$_m$) < 1 for non-metallic nature of solids [18]. In the present investigation, the value of (R$_m$/V$_m$) is found to be ~ 0.63 for all TWGCex glasses indicating their non-metallic nature. The increased concentration of Ce^{3+} ions (C) cause a decrease in inter-ionic distance (r$_i$) resulting to energy transfer among the excited Ce^{3+} ions at higher concentrations.

In order to evaluate the optical band gap energy of prepared TWGCex glass samples, the room temperature optical absorption spectra were measured and presented in Fig. 1c. The optical band gap energy is one of

Table 1
Comparison of basic parameters of TWGCex glasses.

Parameter	TWGCe0	TWGCe0.1	TWGCe0.5	TWGCe1.0
Optical path length, $l \pm$ 0.01 cm	0.18	0.18	0.18	0.18
Density, d $\pm$ 0.001 g/cm^3	4.454	5.067	5.086	5.102
Refractive index, n $\pm$ 0.001	2.448	2.453	2.458	2.462
Reflection losses, R$_L \pm$ 0.02 %	~18	~18	~18	~18
Molar refraction, R$_m \pm$ 0.01 cm^3	22.12	19.48	19.45	19.42
Molar volume, V$_m \pm$ 0.01 cm^3	35.41	31.13	31.02	30.94
(R$_m$ / V$_m$) $\pm$ 0.02	~0.63	~0.63	~0.63	~0.63
Concentration, C $\pm$ 0.02 $\times$ 10^{20} ions/cm^3	–	1.10	5.53	11.03
Inter-ionic distance, r$_i \pm$ 0.01 Å	–	20.84	12.18	9.68
Indirect band gap energy, E$_g \pm$ 0.02 eV	2.56	2.40	2.24	2.16
Direct band gap energy, E$_g \pm$ 0.02 eV	2.84	2.74	2.54	2.42
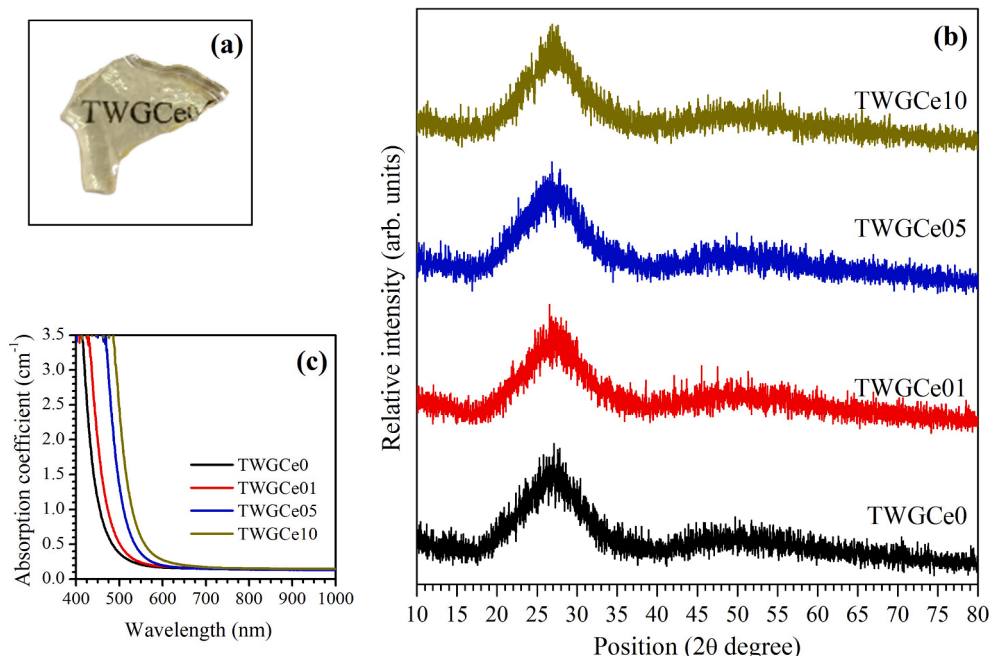
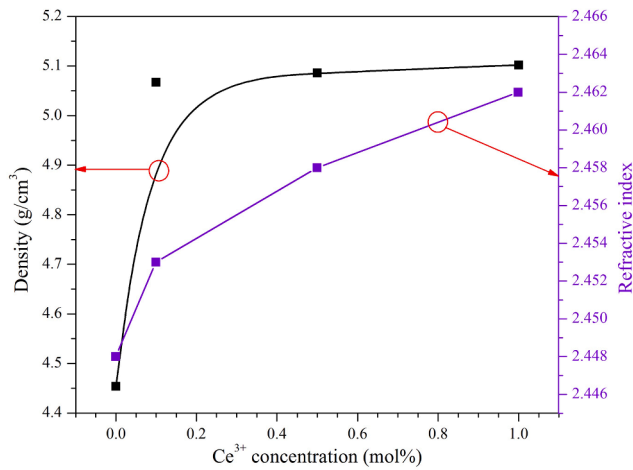**Fig. 1.** Image of TWGCe05 glass (a), XRD profiles(b) and absorption spectra (c) of TWGCex glasses.

Fig. 2. Variation of density and refractive index of TWGCe*x* glasses as a function of Ce³⁺ concentration.

the significant properties to analyze the optical transitions of active ions doped in a glassy matrix and it can be determined using UV–VISabsorption spectra (see Fig. 1**c**). The absorption coefficient (α = Absorbance /optical path length) near the absorption edge and the photon energy (h*ν*)of incident radiation are related as shown below [19].

$$\alpha \cdot (h\nu) \ = \ B (h\nu - E_{opt})^{q} \tag{1}$$

where B is a constant and it is independent of photon energy. The integer q represents the type of transition (direct/indirect) and it has 1/2, 1/3, 2 and 3 for direct allowed, direct forbidden, indirect allowed and indirect forbidden transitions, respectively. This condition is applicable under negligible reflectance. In case of glassy material, the reflectance can be minimized by polishing them to optically high quality [20–24]. The value of indirect and direct band gap energies has been obtained by extrapolating the linear region of Tauc's plots to meet the h*ν* axis as shown in Fig. 3. In the present investigation, both indirect and direct band gap energies found decrease with increase of Ce³⁺ concentration (see Table 1). The addition of low concentrations of dopant ions

decreases the energy band gap and it could be due to small separation distance between dopant ions [25].

3.2. FTIR and SEM analysis

The FTIR spectra help us to know various structural vibrations present in the glass host. The FTIR spectra of TWGCe0 and TWGCe05 glasses shown in Fig. 4 are similar and they are identical to other tellurite glass [26]. The IR bands at ~ 3437, ~2361 and ~ 1713 cm⁻¹ belongs to the symmetric stretching vibrations of HO⁻ group [5,27], the IR band noticed at ~ 871 cm⁻¹ is related to asymmetric stretching vibrations of Ge-O-Ge and W-O-W units [26]. The bands at ~ 721 and 642 cm⁻¹ have been ascribed to Te-O stretching vibrations in TeO₄ and TeO₃ units respectively [28]. The presence of OH⁻ content influence the luminescence properties of RE active ions in a glassy matrix [29] and it can be evaluated using the equation,$\alpha_{OH} \ = \ \ln(T_0 / T_D) / l$, where T₀ is the maximum transmittance, T_D is transmittance corresponding to 3000 cm⁻¹by assuming the reflectance as zero and *l* is the optical path length.
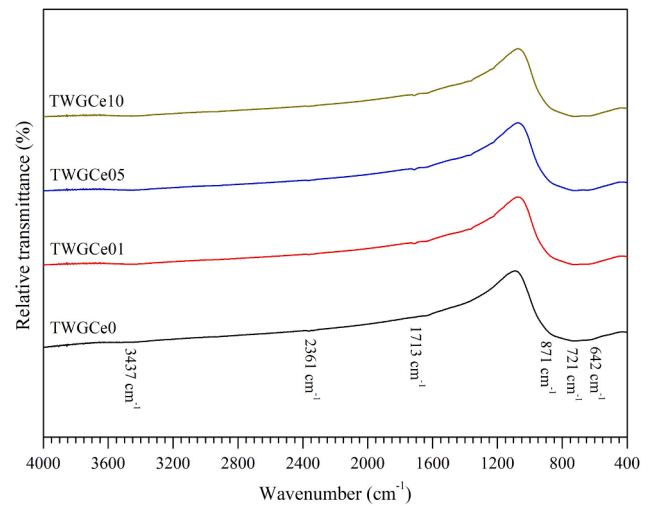

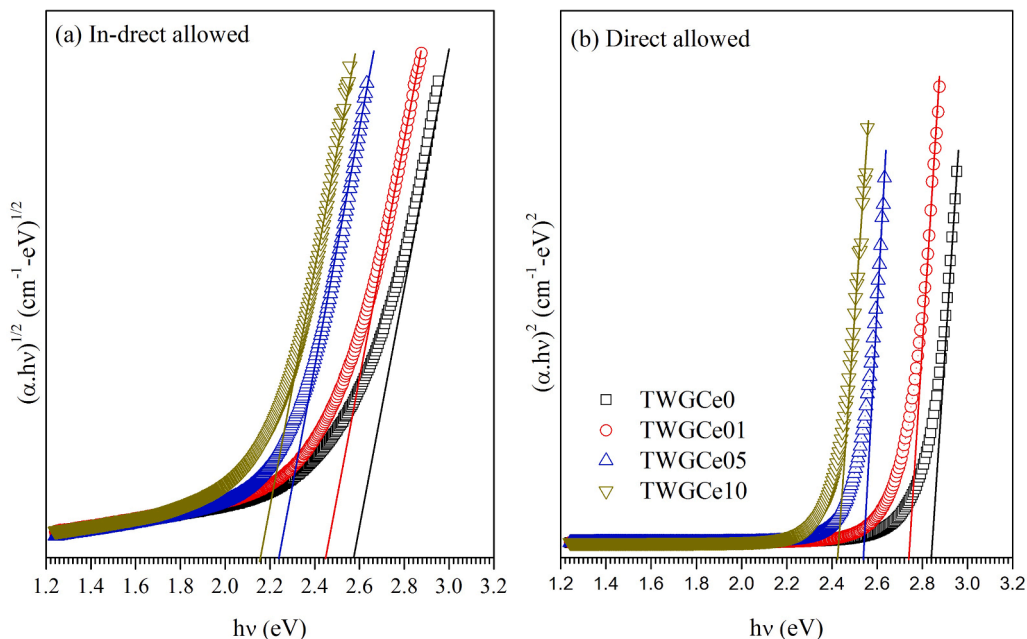**Fig. 4.** FTIR spectra of TWGCe*x* glasses.

Fig. 3. Tauc's plots for indirect (a) and direct (b) allowed transition in TWGCe*x* glasses.

Lower the OH⁻ content lesser will be the non-radiative losses. The value of α_{OH} is found to be 0.51 and 0.48 ± 0.02 cm⁻¹ for TWGCe0 and TWGCe05 glasses, respectively. The addition of Ce_2O_3 content reduces the α_{OH} value resulting to enhance the luminescence properties.

The SEM micrograph with EDS spectrum of TWGCe05 glass is shown in Fig. 5. As can see the SEM micrograph, one can notice that the prepared glass samples have good amorphous phase and they are free from air-bubbles, clusters and defects. The EDS spectrum shows the presence of all elements distributed uniformly indicating the proposed chemical composition. The atomic weight percentages of different elements present in the TWGCe05 glass are 61.77 at%, 4.52 at%, 31.53 at%, 1.69 at% and 0.49 at% for oxygen (O), germanium (Ge), tellurium (Te), tungsten (W) and cerium (Ce) and the corresponding mole percentages are 23.98 mol%, 23.60 mol%, 30.81 mol%, 16.87 mol% and 4.74 mol%.

3.3. Luminescence properties

The excitation and emission spectra of TWGCex glasses are shown in Fig. 6. The excitation spectra monitoring the emission at 408 nm consists of a broad band extended from 243 nm to 360 nm and has been assigned to Ce^{3+}: $4f \rightarrow 5d$ transition [see Fig. 6(a)]. This broad band appears having three sub-peaks with maximum at ∼ 255, ∼274 and ∼ 323 nm. The emission spectra recorded at 323 nm excitation consists of a broad and intense band due to Ce^{3+}: $5d \rightarrow 4f$ (408 nm) transitions. The intensity of excitation band increases with increase of Ce^{3+} concentration, while the intensity of emission bands increases with increase of Ce^{3+} concentration reach to maximum at × = 0.5 mol% and then decrease for further rise of concentration showing luminescencequenching phenomenon beyond × = 0.5 mol% due to energy transfer (ET) among the excited Ce^{3+} ions at higher concentrations. The emission profiles of TWGCe glasses are similar to those reported for gadolinium oxyfluoroborate [5] and P_2O_5-Li_2CO_3-$GdBr_3$-Al_2O_3 [30] glasses.

As can see the normalized emission spectra shown as inset of Fig. 6 (b), one can notice a red-shift in emitted luminescence with increase of Ce^{3+} concentration. The peak maximum of Ce^{3+}: $5d \rightarrow 4f$ transition shifts from 403 nm for × = 0.1 mol% to 408 nm for × = 0.5 mol% and

finally to 410 nm for × = 1.0 mol%. The observed red-shift has been ascribed to the site distribution of Ce^{3+} ions in the ligand fields [31]. It is well known that when the energy of incident light photons is equal or greater than band gap energy of the material then the photons are absorbed by the material and excites the active ions to higher energy levels. When excited at 323 nm wavelength, the ground state Ce^{3+}: $4f$ ions get excited to Ce^{3+}: $5d$ emission state resulting to exhibit intense luminescence through Ce^{3+}: $5d \rightarrow 4f$ transition. The emission mechanism of Ce^{3+} ions in TWGCex glasses at 323 nm excitation is illustrated in Fig. 7(a).

The Commission International de I'Eclairage (CIE-1931) chromaticity coordinates evaluated from the emission spectral profiles have been used to know the colour purity (CP) and correlated colour temperature (CCT) of emitted luminescence. For TWGCex glasses excited at 323 nm, the CIE chromaticity coordinates are obtained as (x = 0.161, y = 0.018).The CP and CCT values have been determined using the equations shown below.

$$CP = \frac{\sqrt{(x - x_e)^2 + (y - y_e^2)}}{\sqrt{(x_d - x_e)^2 + (y_d - y_e^2)}} \times 100 \qquad (2)$$

$$CCT = -449 z^3 + 3525 z^2 - 6823.3 z + 5520.33 \qquad (3)$$

where (x_e, y_e) represents the coordinates of epicenter point and (x_d, y_d) represents the coordinates for dominant-wavelength-point. Generally, the typical coordinates for equal-energy point are (0.333, 0.333). The constant z can be obtained using the formula, z = (x – x_e)/ (y – y_e). The evaluated CIE coordinates are located in the intense blue region of CIE diagram shown in Fig. 7(b). The colour purity is estimated to be 98 % and the corresponding CCT rating is 1802 K. It is well known that the light sources with CCT < 3000 K emit warm light useful for living room illumination. It is known that the generation of white light from phosphor-based LEDs requires blue light excitation. The observed results show that the studied glasses emits intense and warm blue light suitable for decorative lighting sources as well as replacement for blue light source in phosphor-based w-LEDs.
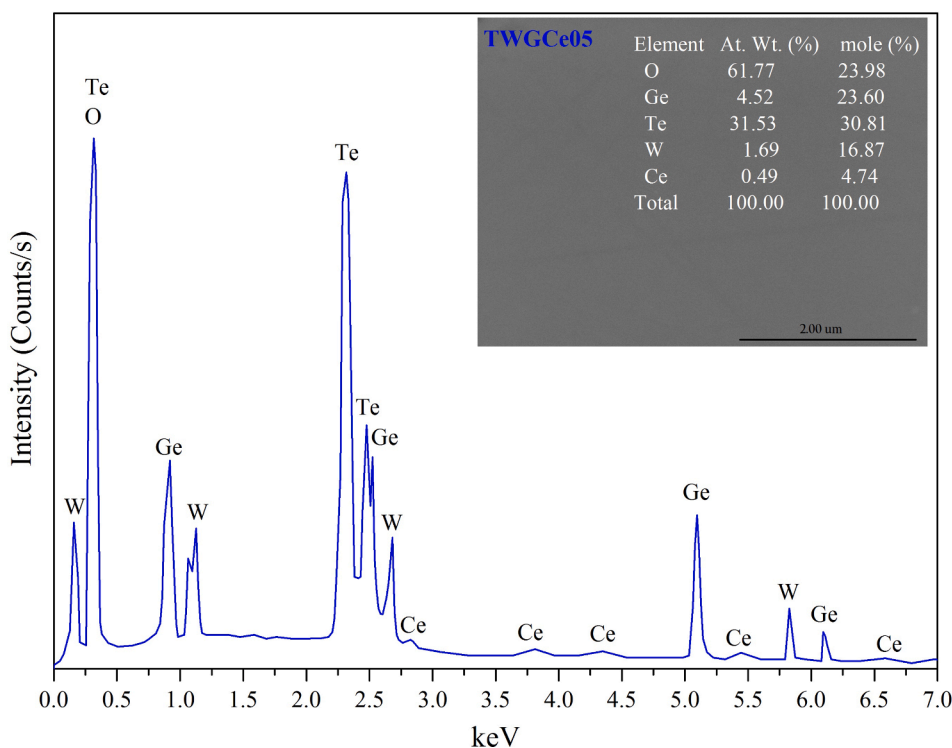

Element	At. Wt. (%)	mole (%)
O	61.77	23.98
Ge	4.52	23.60
Te	31.53	30.81
W	1.69	16.87
Ce	0.49	4.74
Total	100.00	100.00

Fig. 5. EDS profile of TWGCe05 glass. Insets show the SEM micrograph and elemental analysis.
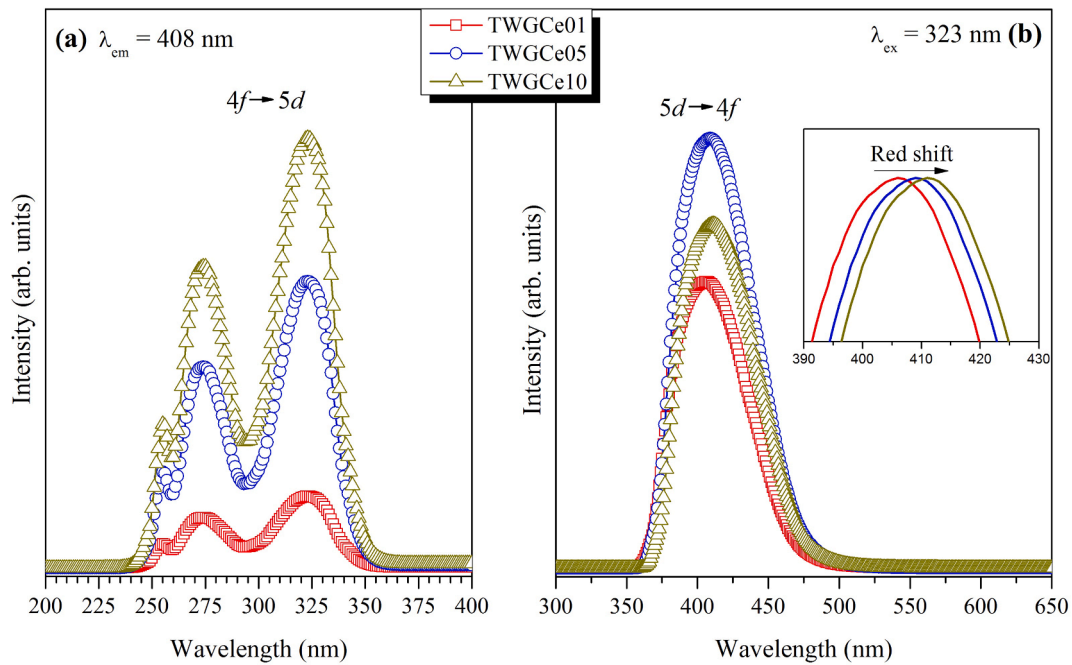
Fig. 6. Excitation (a) and emission (b) spectra of TWGCex glasses. Inset shows a red-shift in emission spectra at 323 nm excitation.
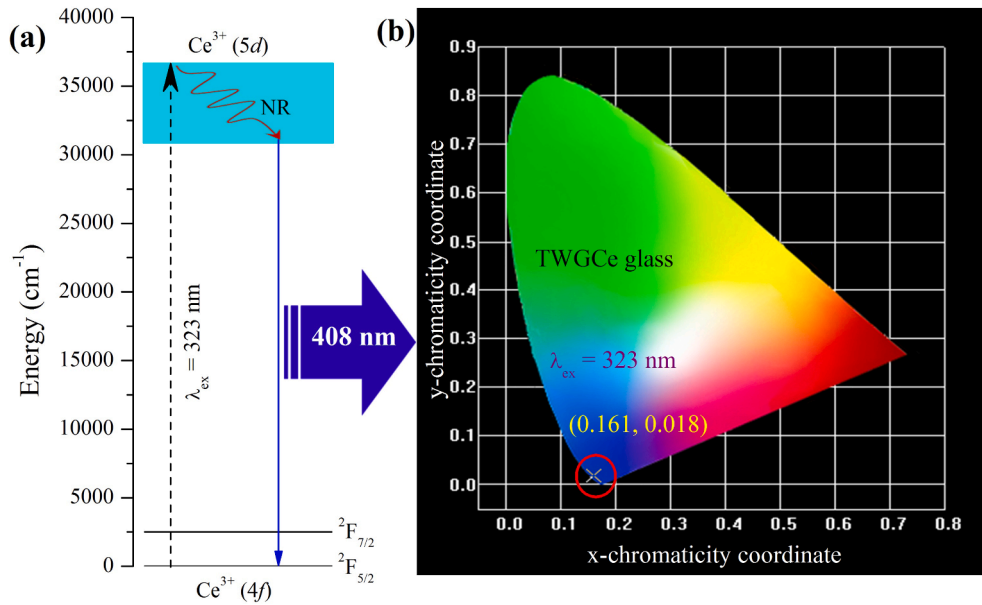

Fig. 7. Emission mechanism of Ce^{3+} ions at 323 nm excitations (a) and the chromaticity diagram of TWGCex glasses.

The process of ET among the excited active ions occurs either due to exchange interaction or multi-polar interaction process depending upon the critical transfer distance but not on inter-ionic distance. According to Dexter's theory of sensitized luminescence in solids [32], the exchange interaction type of ET is possible for $R_c \leq 5$ Å and beyond this limit ($R_c > 5$ Å) the multi-polar interaction come into play for the transfer of energy among the excited ions. The inter-ionic distance (r_i) is the average distance among the sites of Ce^{3+} ions in TWGCe glass host matrix, while the critical transfer distance (R_c) represents the mean distance among the Ce^{3+} ions for which threshold transfer of energy occurs at suitable excitation. The value of R_c responsible for ET mechanism has been estimated using the following formula [33].

$$R_c = \left(\frac{M}{N_A . d . C} \right)^{1/3} \quad (4)$$

where M is the molar mass, N_A is the Avagadro's number, d is the density and C is the concentration of active ions (in g/mol). The value of R_c is found to be 5.56, 3.82 and 3.03 Å for x = 0.1, 0.5 and 1.0 mol%, respectively. These values suggest that the exchange interaction mechanism play a key role in ET for TWGCex glasses.

3.4. Luminescence decay

The luminescence decay curves of Ce^{3+} in TWGCex glasses monitoring the emission and excitation wavelengths at 408 nm and 323 nm

respectively are illustrated in Fig. 8. These decay curves are well fitted to a double exponential function, $I(t) = A_1 \cdot e^{-t/\tau_1} + A_2 \cdot e^{-t/\tau_2}$, where I(t) represent the emission intensity as a function of time t, A_1 & A_2 are constants and τ_1 & τ_2 are the short and long decay times, respectively. The average decay time $\langle\tau\rangle$ has been estimated using well known equation, $\langle\tau\rangle = \frac{A_1 \cdot \tau_1^2 + A_2 \cdot \tau_2^2}{A_1 \cdot \tau_1 + A_2 \cdot \tau_2}$. In the present case, the values of $\langle\tau\rangle$ are determined as 23.92, 22.15 and 19.32 ns for TWGCe0.1, TWGCe0.5 and TWGCe1.0 glasses, respectively. The gradual decrease in decay time with the addition of Ce^{3+} ions in TWG glass host is an indication of energy transfer among the excited Ce^{3+} ions at higher concentrations.

4. Conclusions

The TWGCe*x* glasses have been prepared with perfect amorphous phase by conventional melt-quench method are free from bubbles and impurities. The ratio of molar refraction to molar volume is found lesser than unity $[(R_m/V_m) > 1]$ showing non-metallic nature of TWGCe*x* glasses. The OH^- content of the order $0.51 - 0.48$ cm^{-1} is favourable to improve the luminescence properties. The SEM micrograph confirms the absence of impurities and bubbles and the EDS results show the presence of all the elements distributed uniformly. These glasses exhibit deep-blue luminescence through Ce^{3+}: $5d \rightarrow 4f$ transition when excited at 323 nm wavelength. The observed concentration quenching has been ascribed to the exchange interaction among the excited Ce^{3+} ions at higher concentrations. For all TWGCe*x* glasses, the lifetime is found to be 1.02 ns. The colour perception and CCT rating values are found to be 99 % and 1802 K, respectively are more favourable for decorative lighting sources. The intense and fast luminescence signal is more suitable to be used as a scintillator material. The observed results suggest that the TWGCe05 glass is more favourable to design decorative blue light sources for living rooms and a suitable blue light source to design w-LEDs.
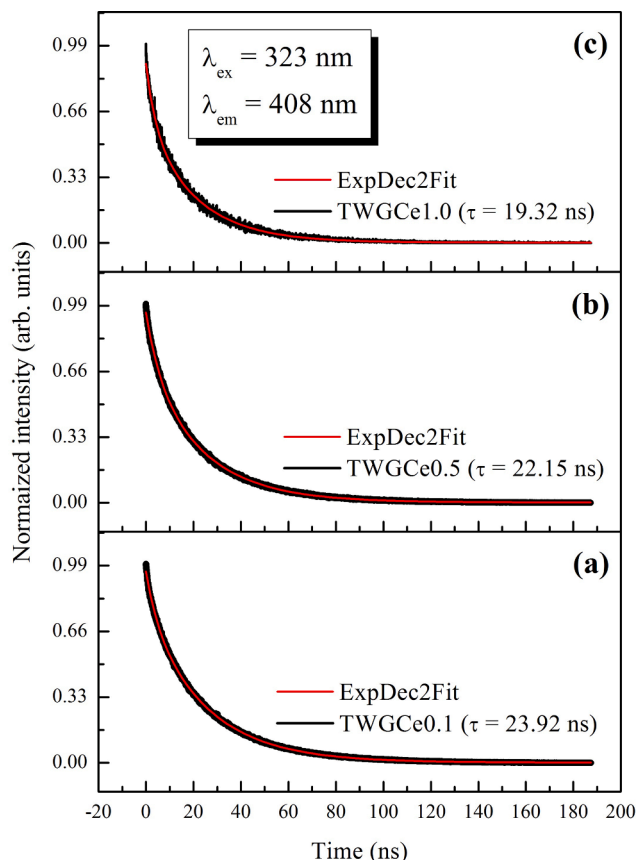
CRediT authorship contribution statement

G. Pullaiah: Methodology, Writing – original draft. **K. Venkata Rao:** Software, Investigation, Writing – review & editing, Supervision. **B.C. Jamalaiah:** Conceptualization, Software, Investigation, Writing – review & editing. **N. Madhu:** Software, Validation, Writing – review & editing. **Venkatramaiah Nutalapati:** Validation, Writing – review & editing.

Declaration of Competing Interest

The authors declare that they have no known competing financial interests or personal relationships that could have appeared to influence the work reported in this paper.

Data Availability Statement

Data will be made available on reasonable request.

References

[1] X.Y. Suna, X.J. Liua, Y. Wu, Z. Xiao, Q. Chen, W.F. Wang, Q.M. Yang, Enhanced emission intensity of Ce^{3+}-doped aluminoborosilicate glasses prepared in air, Ceram. Int. 46 (2020) 4035–4038, https://doi.org/10.1016/j.ceramint.2019.10.109.

[2] Y. Tratsiak, E. Trusova, G. Dosovitsky, M. Fasoli, M. Korjik, F. Moretti, A. Vedda, Photo- and radio-luminescence properties of $3CaO \cdot 2SiO_2$ and $3CaF_2 \cdot 2SiO_2$ glasses doped by Ce^{3+} ions, J. Lumin. 188 (2017) 289–294, https://doi.org/10.1016/j.jlumin.2017.04.051.

[3] F. El-Diasty, F.A. Abdel Wahab, M. Abdel-Baki, Optical band gap studies on lithium aluminum silicate glasses doped with Cr^{3+} ions, J. Appl. Phys. 100 (9) (2006) 093511.

[4] H. Zheng, D. Gao, X. Zhang, E. He, X. Zhang, Fluorescence characteristics of Tm^{3+} in different local environments, J. Appl. Phys. 104 (1) (2008) 013506.

[5] N. Wantana, Y. Ruangtaweep, E. Kaewnuam, S. Kothan, A. Prasatkhetragarn, J. Kaewkhao, Strong emission from Ce^{3+} doped gadolinium oxyfluoroborate scintillation glasses matrix, Rad. Phys. Chem. 185 (2021), 109497, https://doi.org/10.1016/j.radphyschem.2021.109497.

[6] R. Buczynski, J. Pniewski, D. Pysz, R. Stepien, R. Kasztelanic, I. Kujawa, A. Filipkowski, A. Waddie, M. Taghizadeh, Dispersion management in soft glass all-solid photonic crystal fibres, Optoelect. Rev. 20 (2012) 207–215, https://doi.org/10.2478/s11772-012-0033-y.

[7] A. Vedda, N. Chiodini, D.D. Martino, M. Fasoli, S. Keffer, A. Lauria, M. Martino, F. Moretti, G. Spinolo, M. Nikl, G. Brambilla, Ce^{3+}-doped fiber for remote radiation dosimetry, Appl. Phys. Lett. 85 (2004) 6356-6358. https://doi.org/10.1063/1.1840127.

[8] N. Wantana, E. Kaewnuam, N. Chanthima, S. Kaewjaeng, H.J. Kim, J. Kaewkhao, Ce^{3+} doped glass for radiation detection material, Ceram. Int. 44 (2018) S172–S176, https://doi.org/10.1016/j.ceramint.2018.08.121.

[9] L. Vijayalakshmi, K. Naveen Kumar, G. Srinivas, J. Pyung Hwang, J. Choi, Ravishing blue emission from Ce3+ activated lithium borate glasses for photonic applications, Optik 227 (2021), https://doi.org/10.1016/j.ijleo.2020.166025.

[10] W. Lei, Z. Luo, Y. He, S. Liu, P. Zhang, H. Liang, A. Lu, Preparation and broadband white emission of Ce^{3+}-doped transparent glass-ceramics containing ZnO nanocrystals for WLEDs applications, J. Alloys Compds. 875 (2021), 159979, https://doi.org/10.1016/j.jallcom.2021.159979.

[11] V.H. Rao, P.S. Prasad, M.M. Babu, P.V. Rao, T. Satyanarayana, L.F. Santos, N. Veeraiah, Spectroscopic studies of Dy^{3+} ion doped tellurite glasses for solid state lasers and white LEDs, Spectrochim. Acta A: Mol. Bio, Spectrosc. 188 (2018) 516–524, https://doi.org/10.1016/j.saa.2017.07.013.

[12] V.P. Tuyen, B. Sengthong, V.X. Quanga, P.V. Do, H.V. Tuyen, L.X. Hung, N. T. Thanh, M. Nogami, T. Hayakawa, B.T. Huy, Dy^{3+} ions as optical probes for studying structure of boro-tellurite glasses, J. Lumin. 178 (2016) 27–33, https://doi.org/10.1016/j.jlumin.2016.05.027.

[13] G. Upender, C.P. Vardhani, S. Suresh, A.M. Awasthi, V.C. Mouli, Structure, physical and thermal properties of WO_3–GeO_2–TeO_2 glasses, Mater. Chem. Phys. 121 (2010) 335–341, https://doi.org/10.1016/j.matchemphys.2010.01.050.

[14] A. Sharma, M.I. Sayyed, O. Agar, H.O. Tekin, Simulation of shielding parameters for TeO_2-WO_3-GeO_2 glasses using FLUKA code, Res. Phys. 13 (2019), 102199, https://doi.org/10.1016/j.rinp.2019.102199.

[15] B.C. Jamalaiah, Intense yellow luminescence from Dy^{3+}-doped TeO_2-WO_3-GeO_2 glasses: Structural and optical characterization, J. Phys. Conden. Matter 30 (33) (2018) 335701.

[16] B.C. Jamalaiah, G. Viswanadha, TeO_2-WO_3-GeO_2-NdF_3 glasses for 1.06 μm fiber lasers: An optical analysis, Opt. Mater. 90 (2019) 99–107, https://doi.org/10.1016/j.optmat.2019.02.031.

Fig. 8. Luminescence decay profiles of TWGCe*x* glasses.

[17] T. Subrahmanyam, K. Rama Gopal, R. Padma Suvarna, B.C. Jamalaiah, Ch. Srinivasa Rao, Optical properties of Sm3+ -doped TeO2-WO3-GeO2glasses for solid state lasers, Physica B: Conden. Matter 533 (2018) 76–82, https://doi.org/10.1016/j.physb.2018.01.007.

[18] K.F. Herzfeld, On atomic properties which make an element a metal, Phys. Rev. 29 (5) (1927) 701–705.

[19] N.F. Mott, E.A. Davis, Electronic processes in non-crystalline materials, 2nd eds. Clarendon Press, New York, 1979, pp. 382-428.

[20] A.A. Ali, Optical properties of Sm^{3+} -doped CaF$_2$ bismuth borate glasses, J. Lumin. 129 (2009) 1314–1319, https://doi.org/10.1016/j.jlumin.2009.06.017.

[21] P. Subbalakshmi, N. Veeraiah, Dielectric dispersion and certain other physical properties of PbO-Ga$_2$O$_3$-P$_2$O$_5$ glass system, Mater. Lett. 56 (2002) 880–888, https://doi.org/10.1016/S0167-577X(02)00631-6.

[22] A. El-Denglawey, A. Dahshan, K.A. Aly, Y.B. Saddeek, Mechanical properties and band gap estimations of stoichiometric GeSe$_2$-As$_2$Se$_3$ glasses, Optik 245 (2021), 167693, https://doi.org/10.1016/j.ijleo.2021.167693.

[23] A. Ramesh Babu, S. Yusub, Ascendancy of iron ions on lithium-ion conductivity, optical band gap, Urbach energy and topology of LiF-SrO-B$_2$O$_3$ glasses, J. Non-Cryst. Solids 533 533 (2020) 119906.

[24] H. Ticha, J. Schwarz, L. Tichy, Raman spectra and optical band gap in some PbO-ZnO-TeO2 glasses, Mater. Chem. Phys. 237 (2019) 121834, https://doi.org/10.1016/j.matchemphys.2019.121834.

[25] A. Shaker, A. Zekry, A new and simple model for plasma- and doping-induced band gap narrowing, J. Electron Devices 8 (2010) 293–299.

[26] A.A. El-Moneim, DTA and IR absorption spectra of vanadium tellurite glasses, Mater. Chem. Phys. 73 (2002) 318–322, https://doi.org/10.1016/S0254-0584(01)00355-8.

[27] S. Hong-Tao, D. Shi-Xun, X.u. Shi-Qing, H.u. Li-Li, J. Zhong-Hong, Frequency Upconversion Emission of Er^{3+}-doped strontium–lead–bismuth glasses, Ch. Phys. Lett. 21 (11) (2004) 2292–2294.

[28] R.A. El-Mallawany, Theoretical and experimental IR spectra of binary rare earth tellurite glasses, Infr. Phys. 29 (1989) 781–785, https://doi.org/10.1016/0020-0891(89)90125-5.

[29] H. Ebendorff-Heidepriem, W. Seeber, D. Ehrt, Dehydration of phosphate glasses, J. Non-Cryst. Solids 163 (1993) 74–80, https://doi.org/10.1016/0022-3093(93)90647-G.

[30] A.V. Ntarisa, S. Saha, P. Aryal, H.J. Kim, A. Khan, N.D. Quang, I.R. Pandey, J. Kaewkhao, S. Kothan, Luminescence and scintillation properties of Ce^{3+} -doped P$_2$O$_5$-Li$_2$CO$_3$-GdBr 3-A$_l$2$_0$3 glasses, J. Non-Cryst. Solids 567 (2021), 120914, https://doi.org/10.1016/j.jnoncrysol.2021.120914.

[31] X.J. Wang, H.R. Zheng, D. Jia, S.H. Huang, R.S. Meltzer, M.J. Dejneka, W.M. Yen, Spectroscopy of different sites in Pr^{3+}-doped oxyfluoride glass ceramics, Microelect. J. 34 (2003) 549–551, https://doi.org/10.1016/S0026-2692(03)00045-4.

[32] D.L. Dexter, A Theory of sensitized luminescence in solids, J. Chem. Phys. 21 (1953) 836–850, https://doi.org/10.1063/1.1699044.

[33] X.-Y. Sun, D.-G. Jiang, S.-W. Chen, G.-T. Zheng, S.-M. Huang, M. Gu, Z.-J. Zhang, J.-T. Zhao, Eu^{3+}-activated borogermanate scintillating glass with a high Gd$_2$O$_3$ Content, J. Am. Ceram. Soc. 96 (2013) 1483–1489, https://doi.org/10.1111/jace.12205.